Rare Metal Materials and Engineering
Volume 49, Issue 11, November 2020
Available online at www.rmme.ac.cn

Science Press

Cite this article as: Rare Metal Materials and Engineering, 2020, 49(11): 3769-3775.

ARTICLE

Hydrogen Embrittlement Behavior and Mechanisms of Ti-6Al-4V Alloy Based on Small Punch Test

Wang Xian, Zhu Rongtao, Li Chaoyong, Wang Xiang, Huang Pengfei

School of Chemical Engineering and Technology, China University of Mining and Technology, Xuzhou 221116, China

Abstract: Ti-6Al-4V (TC4) alloy is widely used in the field of marine and aviation, and its severe service environment is easy to induce hydrogen embrittlement (HE) which can cause the degradation of mechanical properties and a sudden catastrophic fracture for the material. To investigate the HE behavior and mechanisms, mechanical properties of the TC4 alloy after different electrochemical hydrogen charging (EHC) time were measured by small punch test (SPT) first. Then, hydrogen distribution and the phase transition of the TC4 alloy with different EHC time were discussed by the atomic force microscopy (AFM) and X-ray diffraction (XRD) techniques. The strength and elongation obtained from SPT fitting data show obvious deterioration with the increase of EHC time while the macroscopic fracture morphology of the TC4 alloy exhibits a transformation from ductile mode to brittle mode. At the same time, the generation of hydride after EHC is proved a main contributor to the HE of the TC4 alloy. The results in this paper provide an effective and convenient method to assess the HE behavior of TC4 alloy in service.

Key words: Ti-6Al-4V alloy; hydrogen embrittlement; small punch test; hydrogen distribution; phase transition

TC4 alloy is one of the most widely used titanium alloy in marine and nuclear industries, such as in devices of sea water desalination, sea water cooler and nuclear waste disposal. The devices are usually exposed to hydrogen environments, which often degrade the mechanical properties of TC4 alloy due to the action of hydrogen atoms[1], that is, the so-called hydrogen embrittlement (HE). The HE behavior of TC4 alloy seriously affects the safe use and service life of the devices, so it attracts many researchers' attention to ensure the safe operation of the devices[2-5]. Admittedly, lots of methods have been proposed to detect the effect of HE on metal materials in recent years, such as Charpy impact test[6], fracture toughness test[7], slow strain rate tensile test[8]. Although these methods are verified to be effective for evaluating the HE degree, all of them are not suitable to evaluate the HE behavior of in-service device due to the destructive sampling method. Therefore, there is no effective technique or method to solve the problem of nondestructive sampling and reliable HE evaluation for in-service device until the emergence of small punch test (SPT) technology. The SPT technology was developed in the early 1980 s with the aim of estimating the level of deterioration due to irradiation in nuclear vessel steels [9,10]. In recent years, this technology has been used to evaluate HE behavior of different metals by relating the SPT test data with slow strain rate tensile test data[11-16]. For example, Garcia et al[17] studied the effect of HE on the tensile properties of three chromium molybdenum steels (base metal, welding line, heat treated welding line) by SPT method, and the results were correlated with those obtained by conventional standard tensile specimens which proved that SPT can be used to detect the degradation of steel properties caused by hydrogen. Yang et al[18] investigated the HE properties of high strength steel for car use adopting the SPT technique, too. According to experimental results, the maximum load of stress-displacement curve decreases with the increase of hydrogen charging time. Besides, with the elongation of hydrogen time, the quantity of dimple become less which

Received date: November 12, 2019
Foundation item: Fundamental Research Funds for the Central Universities (2019GF08)
Corresponding author: Zhu Rongtao, Ph. D., Professor, School of Chemical Engineering and Technology, China University of Mining and Technology, Xuzhou 221116, P. R. China, Tel: 0086-516-83884442, E-mail: rtzhu2010@cumt.edu.cn

illustrates HE is the main reason that causes this kind of phenomenon [19, 20]. To sum up, they proved that SPT method is a feasible technique to evaluate the HE behavior of metal materials in hydrogen environment. However, there are few reports which focus on HE behavior of TC4 alloy obtained by SPT technique and the study about impact of hydrogen distribution and phase transition in TC4 alloy on the hydrogen behavior is rare, which limits the investigation of HE mechanisms of TC4 alloy. Therefore, detecting the HE behavior of TC4 alloy in service by the SPT technology has drawn forth the attention of our research group. To inspect the HE behaviors and mechanisms of the TC4 alloy, electrochemical hydrogen charging (EHC) with different charging time were carried out first for the TC4 alloy to simulate the service time of the alloy in hydrogen environment, and then the mechanical properties of the TC4 alloy after different EHC time were measured by SPT in this paper. Subsequently, hydrogen distribution and the phase transition in the TC4 alloy were characterized by atomic force microscopy (AFM) and X-ray diffraction (XRD) methods, respectively, and the impact of hydrogen distribution and the phase transition on the HE behavior of the TC4 alloy was discussed. Finally, the microcosmic HE mechanism of the TC4 alloy was predicted in basis of our experimental results. Clearly, the scheme in this paper provides a feasible evaluation method for HE behavior of in-service metal materials in the hydrogen environment.

1 Experiment

The initial sample is the rolled plate of TC4 alloy with 300 mm×150 mm×3 mm size which were first cut into Φ10 mm× 3 mm cylinders by laser cutting. Then these cylinders were cut into Φ 10 mm×0.6 mm circular slices by STX-202A diamond wire cutting machine, after which the surfaces of these circular slices were polished with 1000#、1500#, 2000 # water sandpaper step by step until the desired 0.5 mm thickness was achieved. Afterwards the surfaces of these circular slices were further polished with 0.5 um Al_2O_3 suspension liquid to make it smooth and cleaned with anhydrous C_2H_6O prior to drying in the oven at last.

The as-prepared circular slice samples with diameter of 10 mm and thickness of 0.5 mm were used during the EHC and the samples were marked as A, B, C, D in accordance with the EHC time 0, 2, 8, 16 h, respectively. Before EHC at room temperature, a wire was adhered to the un-hydrogen charging surface of the circular slices samples, and then it was encapsulated with plastic clay to isolate this un-hydrogen charging surface. The EHC device, including a Keithley 2400 precision constant current power supply and an electrobath, which set the sample as the cathode, the platinum as the anode and a 1 mol/L sulfuric acid aqueous solution was used as the electrolytic solution with a current density of 100 mA/cm^2. During the process of EHC, oxygen was generated on the anode surface, and hydrogen was generated on the surface of the TC4 alloy (cathode). Thiourea in the proportion of 2 g/L was added into the electrolyte as a hydrogen poisoning agent to inhibit the recombination of hydrogen atoms into H_2 on the sample surface thereby allowing more hydrogen to enter the TC4 alloy, greatly increasing the hydrogen concentration in the sample [21].

SPT was carried out immediately on an Instron electro-hydraulic servo tension with small punch clamp that is designed according to GB/T 29459.1-2012, GB/T 29459.2-2012 (test method of small punch of metal materials in service for pressure equipment), as shown in Fig.1, after the completion of EHC. In order to improve corrosion resistance, 18Cr-9Ni coating for hydrogen resistance coating on small punch clamp was processed. During the SPT process, considering EHC is an external hydrogenation method which results in the environmental HE of the alloy, and the hydrogen sensitivity of the alloy decreases with the increase of displacement speed, a slower displacement speed of 0.05 mm/min was selected to more fully demonstrate the experimental results. Until the circular slices sample was punctured by the small punch rod which meant the termination of SPT, a load-displacement curve could be recorded from the control computer.

XRD observations were carried out before and after the EHC treatment to reveal the effect of EHC time on the composition of TC4 alloy and make sure if there was hydride generated. Meanwhile, the change of its composition after different EHC treatment time was observed. In addition, fracture morphologies of the TC4 samples with different EHC time were observed by scanning electron microscopy (SEM Quanta 250*) after the SPT and the surface topography image of the TC4 alloy before EHC was measured by Atomic Force Microscope (AFM, Dimension Icon). In the end, Kelvin Probe Force Microscope (KPFM, Dimension Icon) was used to investigate the hydrogen distribution and phase change in the TC4 samples according to the change of the surface work function.

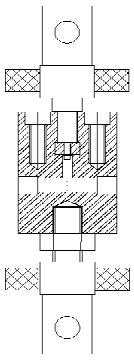

Fig.1 Small punch clamp

2 Results and Discussion

2.1 Composition and microstructure

The main components and the XRD pattern of the TC4 alloy before EHC are illustrated in Table 1 and Fig.2, respectively. Metallographic figure, AFM surface topography image of the original TC4 sample are shown in Fig.3. As shown in Fig.2, the X-ray diffraction pattern for the original TC4 sample has ten broad peaks but only two broad peaks represent β phase which illustrates the content of β phase is far lower that of α phase according to the RIR method (the area of the diffraction peak corresponds to the content of the components and presents a direct proportion relationship)[22]. Similarly, the microstructure of the original TC4 sample shown in Fig.3a also reveal that the original TC4 is composed of a large proportion of equiaxed grains of α phase and a very few nigrescent β phase, which is in agreement with the results of XRD measurement. Besides, the proportion of α phase and β phase observed by metallograph figure are around 80% and 20%, respectively, which is consistent with the results observed by AFM surface topography image shown in Fig.3b.

2.2 Mechanical properties

To obtain the mechanical properties through SPT load-displacement curve, a numerical fitting method should be adopted by the low-strain rate tensile test. Therefore, the fitting equations need to be determined first. To describe the fitting method, the typical plot of the load-displacement curve obtained by SPT test of a ductile metallic alloy with different deformation zones is illustrated in Fig.4. From Fig.4, zone I corresponds to the elastic bending of the sample, along with the indentation produced on its surface by the contact of the head of the punch. Zone II describes the progressive extension of plastic bending to the entire sample.

Table 1 Composition of original TC4 alloy (wt%)

Ti	Al	V	Fe	C	N	H	O
Bal.	5.5	4.0	0.30	0.10	0.05	0.015	0.015

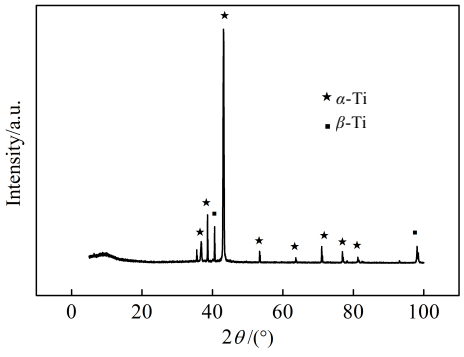

Fig.2 XRD pattern of original TC4 sample

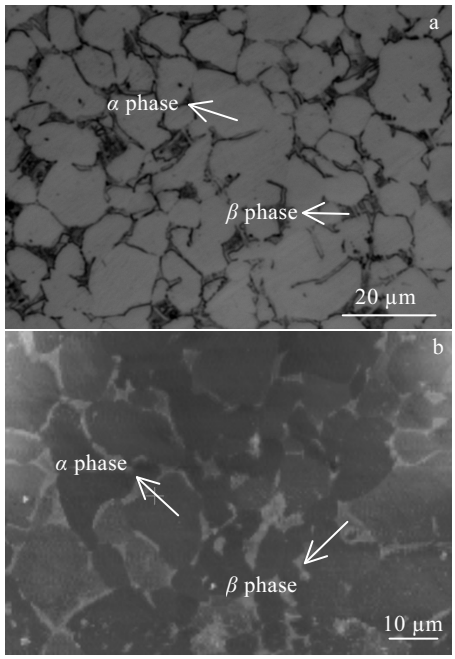

Fig.3 Phase distribution of original TC4 sample: (a) OM image and (b) AFM surface topography image

From a certain moment onward, plastic bending leads to a membrane regime (general plastic deformation), which predominates in most of the curve, and this stage corresponds to Zone III. On approaching the maximum load, the slope of the curve starts to decrease as failure occurs (necking or internal cracking), and the deformation of the sample is in zone IV, where first necking and then a visible crack were finally generated, leading to a decrease in load until total failure of the sample[23].

Based on the deformation behavior in SPT test, the yield strength (σ_{ys}) and the load (P_y) that correspond to the division point of zones I and II have a linear relationship, so σ_{ys} can be calculated by dividing P_y by the square of the initial thickness (d) of the sample. Here we considered that the

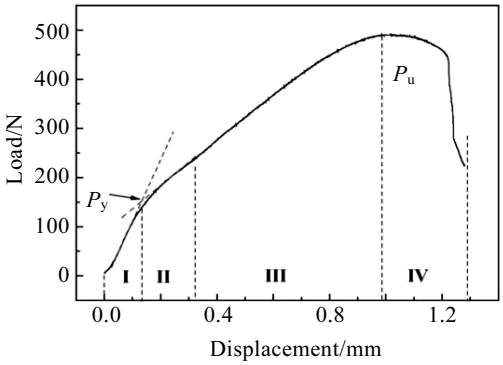

Fig.4 Typical SPT load-displacement curve of the different deformation zones with identification

crossing point of two tangents defined in the elastic regime (zone I) and the plastic regime (zone II) was the yield point of the sample [24], and the yield strength of the SPT sample could be expressed as following through linear fitting [25]:

$$\sigma_{ys} = 0.442 \frac{P_y}{d^2} \quad (1)$$

Similarly, to analyze the relationship between the maximum load of the SPT curve (P_m) and the ultimate strength (σ_{ut}), the linear fitting expressions was also employed in this paper [26].

$$\sigma_{ut} = 0.065 \frac{P_m}{d^2} + 268.81 \quad (2)$$

At the same time, the elongation (A) of the sample in SPT test was also estimated by fitting the displacement (μ_{max}) at the maximum load and tensile elongation of the same sample, so a linear fitting equation was given as follows [27]:

$$A = (0.14375 \mu_{max} / d - 0.2205) \times 100\% \quad (3)$$

The values of P_y, P_m, d_m for the TC4 samples with different EHC time obtained from the load-displacement curves are shown in Fig.5, and the fitted values of yield strength σ_{ys}, ultimate strength σ_{ut} and elongation A of the TC4 samples with different EHC time were calculated based on the equations (1), (2), (3) and listed in Table 2. From Fig.5 and Table 2, the predicted values of the σ_{ys}, σ_{ut} and A of the sample after EHC treatment have a significant reduction compared with those of the non-hydrogenated sample. Obviously, the yield strength (σ_{ys}) reduced by about 11.4%, 21.2%, 39.9% corresponding to the samples hydrogenated for 2 h, 8 h, 16 h, the same trend of elongation (A) was observed for the same EHC time, which indicates that the charging time has a significant effect on the mechanical properties of the TC4 alloy and the TC4 sample exhibits an obvious HE behavior.

To further investigate the HE behavior of the TC4 alloy after EHC, the HE sensitivity of the TC4 alloy was discussed. According to Eq.(4), the sensitivity of hydrogen embrittlement $I_{HE(A)}$ can be obtained according to the change of

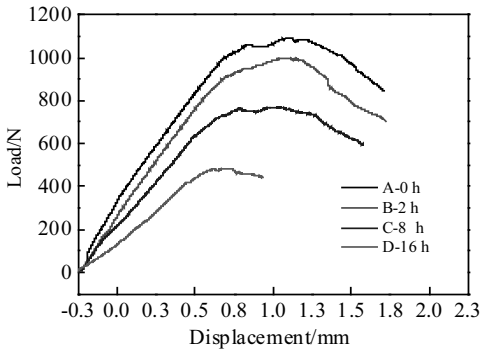

Fig.5 Load-displacement curves of TC4 samples with different EHC time

Table 2 Predicted value of TC4 samples with different EHC time through fitting SPT load-displacement curve

Time/h	0	2	8	16
σ_{ys}/MPa	503.1728	445.8896	396.3856	302.9744
σ_{ut}/MPa	551.43	527.51	466.41	394.39
A/%	11.313	10.056	9.4275	7.542

elongation (A) before and after EHC treatment. A_0 is the elongation of non-hydrogen charged sample, A is the elongation of hydrogen charged sample. Fig.6 shows the change curve of $I_{HE(A)}$ after different EHC time. It can be found that the $I_{HE(A)}$ of TC4 sample has a noticeable improvement from 11.11% to 33.33% with the increase of EHC time, which means that a greater ductile loss is associated with greater susceptibility to hydrogen embrittlement.

$$I_{HE(A)} = \frac{A_0 - A}{A_0} \times 100\% \quad (4)$$

2.3 Hydrogen embrittlement mechanism

As mentioned above, the hydrogenated TC4 sample exhibits an obvious HE sensitivity. Fig.7 shows the SPT fracture morphologies of the TC4 sample after EHC of 2, 8 and 16 h. For comparison, fracture morphologies of the non-hydrogenated sample are given in Fig.7, too. Fig.7a, 7c, 7e, 7g are the overall fracture morphologies of the TC4 sample with different EHC time after SPT. Clearly, the fracture changes from ring shape in non-hydrogenated sample to herringbone shape in hydrogenated sample with the increase of the EHC time, which indicates that deformation of the TC4 alloy transforms from ductile pattern to brittle pattern after EHC treatment. Moreover, Fig.7b, 7d, 7f and 7h show the locally magnified fracture morphologies of the non-hydrogen ated and hydrogenated TC4 samples with different EHC time. Obviously, unevenly distributed dimples are dominantin image of the non-hydrogenated sample (Fig.7b) while the dimples seem to be torn and brittle fracture pattern is presented in the hydrogenated samples (Fig.7d, 7f, 7h). Meanwhile, the

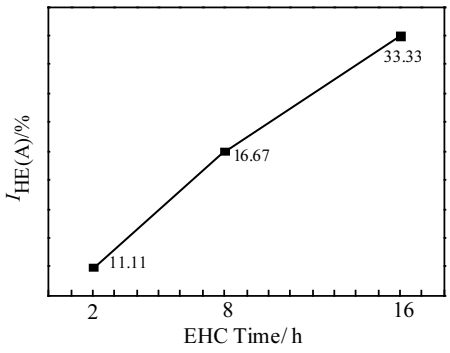

Fig.6 $I_{HE(A)}$ of the TC4 samples with different EHC time after SPT

brittle fracture characteristics of the hydrogenated TC4 alloy become more obvious with the increase of EHC time and a typical fluvial pattern that is a cleavage fault is exhibited in Fig.7f and 7h, which indicates that introduction of hydrogen during the EHC process induces a degradation of plastic deformation of the hydrogenated TC4 alloy; this also can be verified by the mechanical behaviors mentioned in section 2.2.

To inspect the impact of hydrogen on the plastic deformation of the TC4 alloy after introduction of hydrogen during EHC process, KPFM and XRD techniques were used to investigate the hydrogen distribution and phase transition in the samples with different EHC time. The KPFM images of the sample without EHC treatment and with 2, 8, 16 h EHC treatment at room temperature are shown in Fig.8. Clearly, the potential range of selected area has an obvious change after EHC treatment with different EHC time[28-31]. In general, the β phase with body centered cubic (bcc) structure is more sensitive to HE than α phase with close-packed hexagonal (hcp) structure. The diffusion rate of hydrogen in β phase was much higher than that in α phase[32]. It is worth noting that although the potential range increases on both two phases, the β phase always shows higher potential that illustrates the entered hydrogen in TC4 is more concentrated in β phase, which also can be verified by the previous study [33]. Therefore, it can be inferred that hydrogen first permeates into β phase, and precipitates at the interface of the two phases with the increase of the concentration of hydrogen. Meanwhile, it can be seen from the Table 3 that the potential range increases gradually

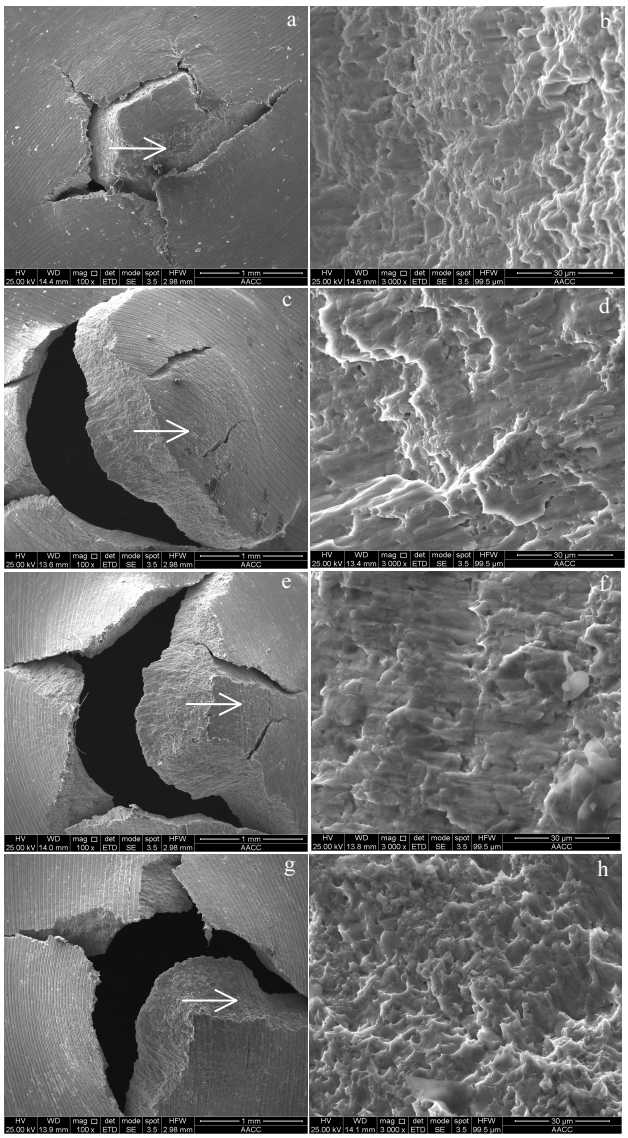

Fig.7 Overall and local fracture SEM images of the non-hydrogenated sample (a, b) and hydrogenated sample with EHC time of 2 h (c, d), 8 h (e, f), and 16 h (g, h)

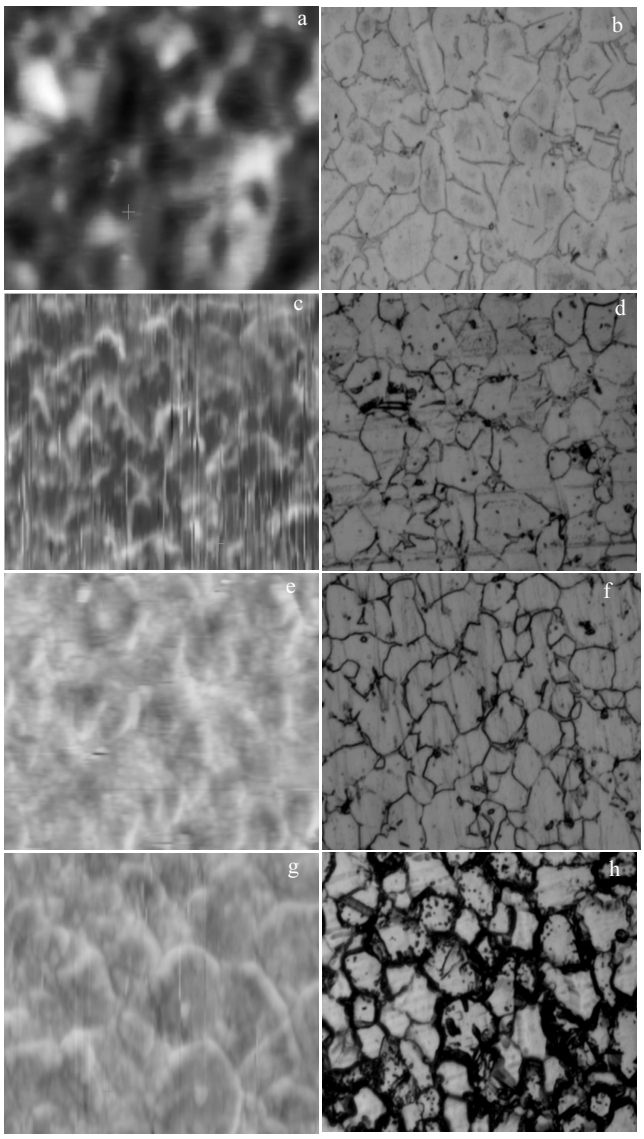

Fig.8 KPFM and metallographic images of TC4 alloy without hydrogenated (a, b) and hydrogenated of 2 h (c, d), 8 h (e, f) and 16 h (g, h)

with the increase of EHC time, and there is not a significant change of potential range in the sample after EHC for 8 and 16 h which means the hydrogen captured by reversible hydrogen trap in TC4 is limited. When the hydrogen captured by reversible hydrogen trap reaches saturation, the potential range will reach a balance point. However, the surface potential range in the TC4 alloy after longer EHC time in Fig.8h is much larger than that in the original sample as shown in Fig.8a, which suggests that hydride that is new phase may be generated after EHC treatment and this hydride cannot decompose at room temperature.

In order to investigate the effect of phase structure change after EHC on the hydrogen embrittlement mechanism in the TC4 alloy, the XRD patterns of the TC4 sample experienced EHC treatment at room temperature are shown in Fig.9. There were γ-TiH and δ-TiH2 hydride generated after EHC treatment when compared to the corresponding pattern of the original TC4 sample shown in Fig.2. At the same time, there is an obvious reduction in β-Ti content, which suggests the hydride maybe grows preferentially in β-Ti. In other words, combining the XRD patterns and metallographic images, hydride originates from the interface between α-Ti and β-Ti and grows up in β-Ti, which results in the reduction of β-Ti content and accumulation of the hydride in the interphase between α-Ti and β-Ti. The generation of the hydride can be confirmed by the KPFM image, for example, Fig.8c. Clearly, compared with the un-hydrogen charged sample, higher surface potential induced by hydride in the interphase between α-Ti and β -Ti can be observed in EHC sample due to the covalent bond in the hydride. Just because of the existence of the hydride as the crack source, TC4 alloy exhibits deteriorated mechanical properties after EHC treatment. Meanwhile, with the increase of EHC time, the free hydrogen that does not react with Ti will promote the crack growth caused by hydride under the SPT, which further leads to the deterioration of the TC4 sample, so the TC4 alloy exhibits a significant HE sensitivity with the increasing EHC time.

Table 3 Potential range of TC4 alloy hydrogenated with different time

Time/h	0	2	8	16
Potential range/V	−0.8~1	−3~2	−4~2	−7~3

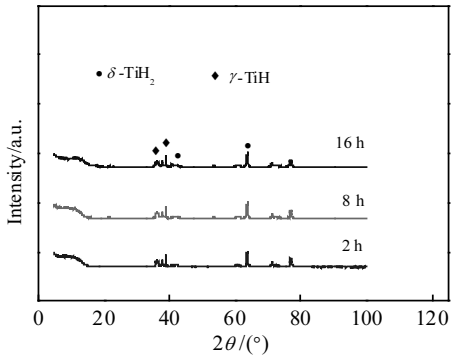

Fig.9 XRD patterns of the TC4 alloy experienced 2, 8, 16 h EHC treatment

3 Conclusions

1) Hydrogen-induced degradation of mechanical properties occurs in TC4 alloy due to EHC treatment, and the TC4 alloy exhibits a severe HE sensitivity with the increase of EHC time.

2) Generation of the hydride during the EHC process, which originates from the interface between α phase and β phase and grows up in β phase, is a main contributor to the HE behavior of the TC4 alloy.

3) The SPT technique combined with KPFM method is a feasible way to assess the HE behavior and mechanism of the TC4 alloy in service.

References

1 Tal-Gutelmacher E, Eliezer D. *Materials Transactions*[J], 2004, 45(5): 1594
2 Tal-Gutelmacher E, Eliezer D, Eylon D *et al*. *Materials Science and Engineering A*[J], 2004, 381(1-2): 230
3 Kim Tae-Kyu, Baek Jong-Hyuk, Choi Byung-Seon *et al*. *Annals of Nuclear Energy*[J], 2002, 29(17): 2041
4 Teter D F, Robertson I M, Birnbaum H K. *Acta Materialia*[J], 2001, 49(20): 4313
5 Mprash K R, Bahr D F. *Scripta Materialia*[J], 2001, 45(7): 839
6 Tavares S S M, Silva M B, deMacêdo M C S *et al*. *Engineering Failure Analysis*[J], 2017, 82: 695
7 Birenis D, Ogawa Y, Matsunaga H *et al*. *Materials Science and Engineering A*[J], 2019, 756(22): 396
8 García T E, Rodríguez C, Belzunce F J *et al*. *Journal of Alloys and Compounds*[J], 2014, 582(5): 708
9 Manahan M P, Argon A S, Harling O K. *Journal of Nuclear Materials*[J],1981, 104: 1545
10 Mao X, Takahashi H. *Journal of Nuclear Materials*[J], 1987, 150: 42
11 Arroyo B, Álvarez J A, Lacalle R *et al*. *Proceedings of 3rd International Conference SSTT*[C]. Graz, Austria: SSTT, 2014
12 Misawa T, Hamaguchi Y, Saito M. *Journal of Nuclear Materials* [J], 1988, 155-157: 749
13 Komazaki S I, Koyama A, Misawa T. *Materials Transactions*[J], 2002, 43(9): 2213
14 T Nambu, K Shimizu,Y Matsumoto *et al*. *Journal of Alloys and Compounds*[J], 2007, 446-447(31): 588
15 Matsumoto Y, Yukawa H, Nambu T. *Proceedings of the 1st International Conference SSTT*[C]. Ostrava: SSTT, 2010
16 García T E, Rodríguez C, Belzunce F J *et al*. *Materials Science and Engineering A*[J], 2015, 626(25): 342

17 García T E, Rodríguez C, Belzunce F J. *Materials Science and Engineering A*[J], 2016, 664: 165
18 Yang S S, Xiang Y C, Qian L Y. *Journal of Alloys and Compounds*[J], 2017, 695: 2499
19 Arroyo B, Álvarez J A, Lacalle R *et al*. *Materials Science and Engineering A*[J], 2017, 691: 180
20 Roger C, Hurst R, Lancaster J *et al*. *Theoretical and Applied Fracture Mechanics*[J], 2016, 86: 69
21 Pereira P A S, Franco C S G, Filho J L M G *et al*. *International Journal of Hydrogen Energy*[J], 2015, 40(47): 17136
22 Ramírez B, Bucio L. *Cellulose*[J], 2018, 25(5): 2795
23 García T E, Rodríguez C, Belzunce F J *et al*. *Journal of Alloys and Compounds*[J], 2014, 582: 708
24 Dobeš F F, Dymáček P, Besterci M. *Materials Science and Engineering A*[J], 2015, 626: 313
25 García T E, Rodríguez C, Belzunce F J *et al*. *Journal of Alloys and Compounds*[J], 2014, 582: 708
26 Mao X, Takahashi H. *Journal of Nuclear Materials*[J], 1987, 150: 42
27 Fleury E, Ha J S. *International Journal of Pressure Vessels and Piping*[J], 1998,75: 699
28 Tehranchi A, Curtin W A. *Journal of the Mechanics and Physics of Solids*[J], 2017, 101: 150
29 Zhu T, Li J, Yip S. *Physical Review Letters*[J], 2004, 93(2): 025 503
30 Zhu T, Li J, Yip S. *Physical Review Letters*[J], 2004, 93(20): 205 504
31 Saintier N, Awane T, Olive J M *et al*. *International Journal of Hydrogen Energy*[J], 2011, 36: 8630
32 Eliezer D, Tal-Gutelmacher E, Cross C E *et al*. *Materials Science and Engineering A*[J], 2006, 433: 298
33 Hua Zhengli, Zhu Shengyi, An Bai *et al*. *Scripta Materialia*[J], 2019,162: 219

基于小冲杆试验的 TC4 合金氢脆行为和机理研究

王　贤，朱荣涛，李超永，王　香，黄鹏飞
(中国矿业大学 化工学院, 江苏 徐州 221116)

摘　要：Ti-6Al-4V (TC4) 合金广泛应用于海洋和航空领域，其恶劣的使用环境容易引发氢脆(HE)失效而使得 TC4 的机械性能退化，导致突然的灾难性断裂。为了研究 TC4 合金的氢脆行为和机理，首先采用小冲杆试验(SPT)测试了 TC4 合金在不同充氢时间下的力学性能。然后, 利用原子力显微镜(AFM)和 X 射线衍射(XRD)仪对 TC4 合金在不同充氢时间下的氢分布和相转变进行了研究。小冲杆试验（SPT）拟合数据显示，随着充氢时间的增加，TC4 合金的强度和伸长率均发生明显的劣化，同时其宏观断口形态由韧性向脆性转变。与此同时，还证明了电解充氢后氢化物的生成是导致 TC4 合金氢脆现象产生的主要原因。本研究结果为在役 TC4 设备的氢脆性能检测提供了一种有效、简便的方法。

关键词：TC4 合金；氢脆；小冲杆试验；氢分布；相转变

作者简介：王　贤，女，1994 年生，硕士生，中国矿业大学化工学院，江苏　徐州　221116，电话：0516-83591063，E-mail: wangxian941109@126.com